Title

Energy of Oxygen-Vacancy Formation on Oxide Surfaces: Role of the Spatial Distribution

Journal

The Journal of Physical Chemistry C, 120(4)

ISSN

1932-7447

Authors

Agarwal, Vishal
Metiu, Horia

Publication Date

2016-02-04

DOI

10.1021/acs.jpcc.5b12054

Energy of Oxygen-Vacancy Formation on Oxide Surfaces: Role of the Spatial Distribution

Vishal Agarwal and Horia Metiu*

Department of Chemistry and Biochemistry, University of California,

Santa Barbara, CA 93106-9510 United States

* Telephone: 805-893-2256. Fax: 805-893-4120. E-mail: metiu@chem.ucsb.edu

Abstract

Oxygen vacancy formation energies are often used as a descriptor of the catalytic activity of metal oxides for oxidation reactions having the Mars-van Krevelen mechanism. When these energies are calculated, it is often assumed that they depend only on the concentration of the vacancies in the top oxygen layer. Previous work has shown that in the case of TiO_2 and V_2O_5, the energy of vacancy formation depends not only on their concentration but also on the manner in which they are distributed on the surface. However the energy change due to the change of configuration in these systems is very small. Here we find that in the case of α-MoO_3(010) the dependence on the energy of vacancy formation of the distribution of vacancies is very large: if the lattice made by the vacancies consists of parallelograms, the energy of vacancy formation is 0.4 eV smaller than when the lattice consists of rectangles (the two systems having the same vacancy concentration).

1. Introduction. Oxides are used as catalysts for partial oxidation reactions.[1-3] It is generally accepted that these reactions proceed through the Mars-van Krevelen mechanism,[4-6] which asserts that the oxygen atoms present in the products originate from the surface of the oxide; the role of the gaseous oxygen in the feed is to reoxidize the oxide. In all cases we are aware of, the reoxidation of the surface is very rapid, and it is not a factor in the overall oxidation kinetics. Because of this it has often been assumed[7-9] that the energy required for making an oxygen vacancy is a good descriptor of the oxidizing power of an oxide: a lower energy of vacancy formation means a better oxidant. This assumption has stimulated a substantial amount of work that calculated the energy of oxygen vacancy formation on various crystalline faces of a large number of oxides. The interest in oxygen vacancy formation is increased by the fact that in many cases they affect the electronic and optical properties of oxides.

Many calculations have shown that the energy to make a vacancy depends on vacancy concentration. This dependence has been studied by calculating how the energy of vacancy formation changes with the size of the supercell used in the computation; because of periodic boundary conditions, a larger supercell means a lower vacancy concentration. Implied in this procedure is the assumption that the energy of a periodic array of oxygen vacancies *depends only on concentration*. Since the single-crystal oxide surfaces are anisotropic, one suspects that the energy of vacancy formation will also depend on the manner in which they are distributed on the surface. The energy of forming the same vacancy concentration may be different if the vacancies are arranged differently on the surface.

The effect of spatial distribution of vacancies on oxygen vacancy formation energies has been discussed previously for TiO_2 [10] and for V_2O_5.[11-12] In both cases the change in the energy of vacancy formation when the distribution was changed, without changing the concentration,

was surprisingly small (less than 0.1 eV for TiO_2 and less than 0.12 eV for V_2O_5). Here we show that in the case of α-MoO_3(010), the energy dependence on the distribution of vacancies is very large. In particular, the energy of vacancy formation when we use parallelogram supercell is smaller by 0.4 eV/per vacancy than when we use a rectangular supercell, even though in both cases we remove one out of sixteen surface oxygen atoms. We use α-MoO_3(010) as an example, because molybdenum oxide is used as a partial oxidation catalyst.[13-14]

2. Computational methodology. We used the VASP program[15-18] for total energy and equilibrium geometry calculations with the PBE+U functional,[19] the projector-augmented-wave (PAW) method[20] and the Grimme's D2 method to include van der Waals interactions.[21] All calculations were performed with spin-polarized DFT. The supercell consists of 4×1×4 unit cells with a vacuum layer of 12 Å. Our simulation cell contains 32 Mo atoms and 96 O atoms. Calculations using HSE06 hybrid functional are prohibitively expensive for the large unit cell considered here. Therefore, we used U = 2 eV (for the *d*-orbitals of Mo atoms) because it gave the best fit to the experimental energy of the reaction $MoO_3 + H_2 \rightarrow MoO_2 + H_2O$, to the measured unit cell parameters, and to the magnetic moments of Mo in MoO_2 (which were calculated with the HSE06 hybrid functional). We varied the k-point mesh until the energy of vacancy formation was converged. The energy cut-off was 400 eV, which was tested by showing that a few calculations using 500 eV give the same total energies. The MoO_3 slab used in all calculations has one MoO_3 bilayer. The bilayers in a MoO_3 crystal interact weakly through van der Waals interactions; a few calculations with two bilayers gave the same results as the ones with one bilayer. The energy of oxygen vacancy formation ΔE_O was calculated by using the equation $\Delta E_0 = E_{vac} + \frac{1}{2}E_{O2} - E_{st}$ where E_{O2} is the energy of the gas phase O_2 molecule, E_{vac} is

the energy of a (010) surface with one oxygen vacancy per supercell, and E_{st} is the energy of the same supercell with no vacancy. Since we compare the energy of vacancy formation for two supercells the difference between these two energies is not affected by the DFT error in calculating the binding energy of O_2.

3. Results and Discussion. The (010) face of α-MoO_3 has three different kinds of oxygen atoms, labelled O_t, O_a and O_s in Figure 1. The easiest to remove (to make an oxygen vacancy) are O_a and O_t and their removal results in the same final state geometry; therefore they are equivalent as far as vacancy formation is concerned. In what follows we discuss the vacancy formed by removing O_a (Figure 1b). In doing this we remove one out of sixteen oxygen atoms present in the surface layer of the supercell.

It is possible to use in the calculations two supercells having different shape but containing the same number of oxygen atoms. Fig. 1a shows a rectangular supercell and Fig. 1b shows a supercell whose shape is a parallelogram. The periodic arrangement of the vacancies for the two supercells is shown schematically in Figs. 2a and 2b. The concentrations of vacancies in the two figures is the same but they differ only through the manner in which they are arranged. Depending on the shape of the supercell used in the DFT calculations, the vacancies form a lattice with whose unit cell is a rectangle or parallelogram (Figs. 2a and 2b). The formation of a rectangular array of vacancies requires 2.57 eV per supercell; this is larger by 0.4 eV (per supercell) than the energy of forming a “parallelogram lattice”. This is a substantial difference which shows that the manner in which the vacancies are distributed matters.

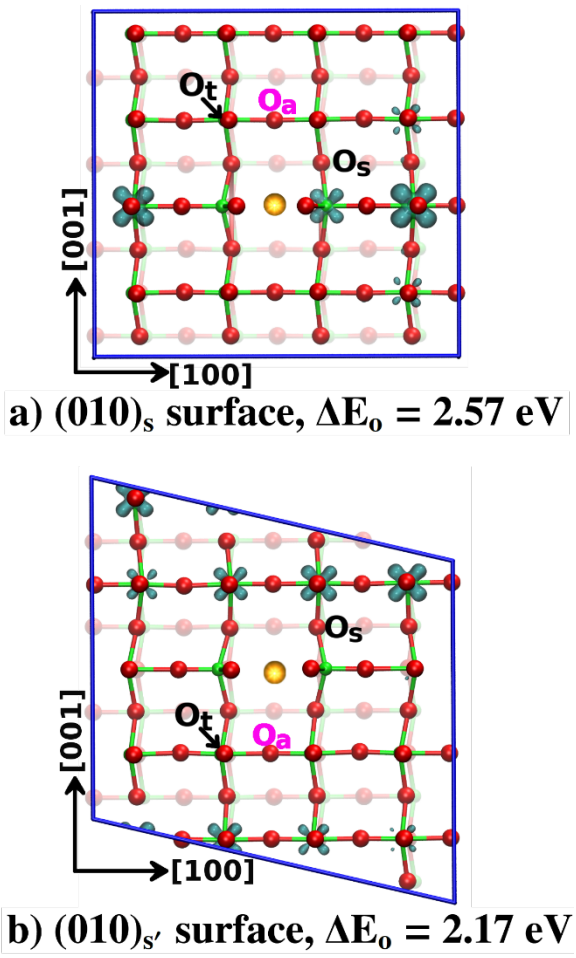

Figure 1. The two supercells used for calculating the energy of oxygen vacancy formation: **(a)** the rectangle supercell and the HOMO orbital created when the oxygen vacancy is formed; **(b)** the parallelogram supercell and the HOMO created when the vacancy is formed. The oxygen atoms are red and the Mo atoms are green (they are not visible because they are obstructed by the oxygen, but their presence is indicated by the green lines coming out of them). The site of the oxygen vacancy is colored yellow. There are three kinds of oxygens on the (010) surface, labeled O_a, O_t and O_s. The removal of O_a, to make an oxygen vacancy, requires the least energy (this is given in the figure).

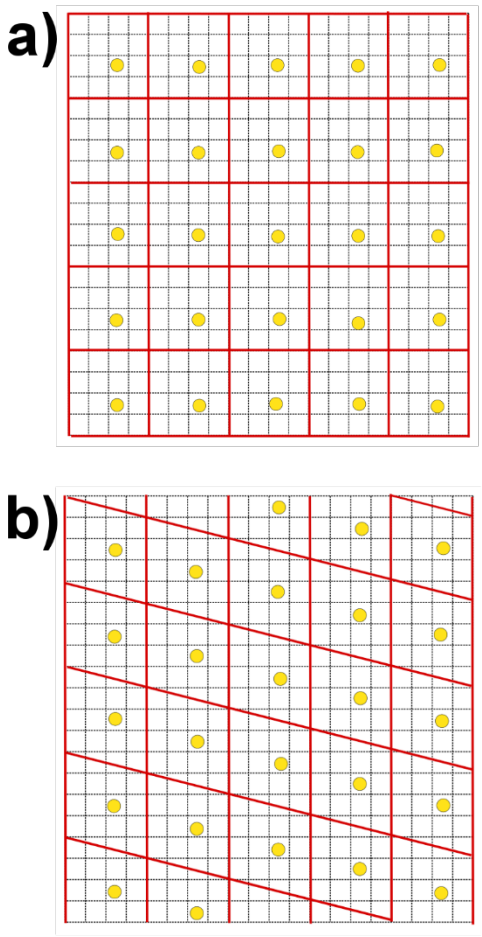

Figure 2. A schematic representation of the distribution of oxygen vacancies **(a)** when the supercell is a rectangle and **(b)** when the supercell is a parallelogram.

Some insight into the reason for these differences is provided by the examination of the highest-occupied molecular orbital (HOMO) for the surface having an oxygen vacancy per supercell. The removal of an oxygen atom from the surface leaves behind two unpaired electrons. For a reducible oxide, such as titania,[22-24] ceria,[25-27] or vanadia,[28-29] these electrons will reduce two cations. For example, forming an oxygen vacancy in TiO_2(110) reduces two Ti cations, from a formal charge of Ti^{4+}, to form two polarons in which titanium has a formal charge

of Ti^{3+}.[22-23, 30] Based on these prior findings one would expect to observe a similar behavior in MoO_3 since Mo is a reducible cation. This is what we find when O_s is removed: the two unpaired electrons left behind are localized on two Mo atoms reducing them (formally) from Mo^{6+} to Mo^{5+}. However, when O_a (or O_t) is removed the HOMO of the reduced surface is delocalized and its shape depends on the shape of the supercell: it is more delocalized when the supercell is a parallelogram. We expect that a more delocalized orbital will have lower energy and this is confirmed by comparing the density of states of the two systems (Figure 3). Figure 3 shows only the orbitals whose energy is in the band gap and which are degenerate: each state is occupied by two electrons. The HOMO of the parallelogram lattice has a lower energy than the HOMO of the rectangular lattice and this is one of the reasons why the parallelogram lattice has a lower total energy than the rectangular one. In addition, we find that in the rectangle lattice the presence of the vacancy disrupts strongly the bonds in the [100] direction (see Figure 4), which indicates the presence of an anisotropic strain. Less strain is observed in the parallelogram structure, which is another possible reason why this structure has lower energy.

Our main conclusion is that the energy of formation of a periodic array of vacancies in the surface layer of an oxide depends on both the surface concentration and on the spatial distribution of the vacancies: surfaces having the same oxygen vacancy concentration can have very different energies if they are distributed differently on the surface. This effect is much larger for the α-MoO_3(010) surface than it is for TiO_2 or CeO_2.

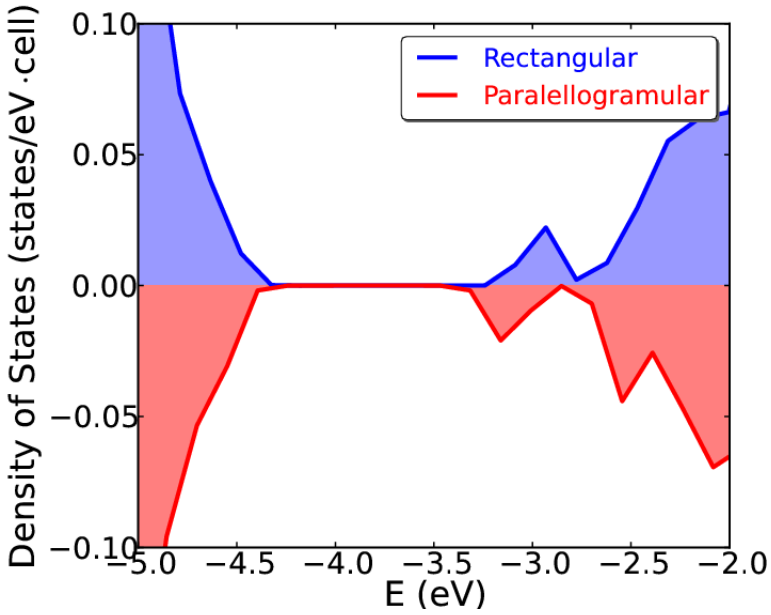

Figure 3. The density of states (DOS) of α-MoO_3(010) having an oxygen vacancy per supercell. The blue shows the density of states for a parallelogram configuration of vacancies and the red shows the DOS for the rectangle configuration. The orbitals in the gap are the HOMOs occupied by the unpaired electrons left behind when O was removed from the surface. The shape and the location of the orbitals are shown in Figure 1.

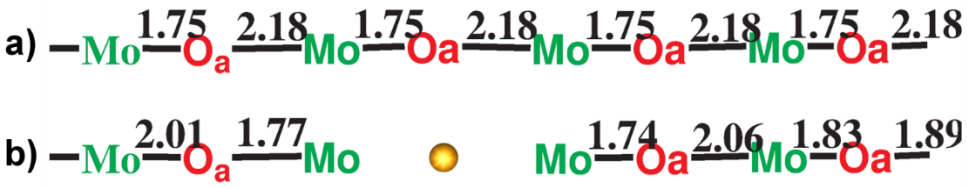

Figure 4. (a) Schematic figure of bond lengths along [100] direction in the rectangular supercell with *no vacancy*. **(b)** Schematic figure of bond lengths along [100] direction in the rectangular supercell with oxygen vacancy. The vacancy is shown in yellow and bond lengths given in Å.

Acknowledgments. VA thanks Dr. Henrik Kristoffersen for stimulating discussions. Financial support was provided by the Department of Energy, Office of Science, Office of Basic Energy Sciences DE-FG03-89ER14048 and the Air Force Office of Scientific Research FA9550-12-1-0147. We acknowledge support from the Center for Scientific Computing at the California NanoSystems Institute and the UCSB Materials Research Laboratory (an NSF MRSEC, DMR-1121053) funded in part by NSF CNS-0960316 and Hewlett-Packard. Use of the Center for Nanoscale Materials was supported by the U.S. Department of Energy, Office of Science, Office of Basic Energy Sciences, under Contract DE-AC02-06CH11357.

References

(1) Centi, G.; Cavani, F.; Trifirò, F. *Selective Oxidation by Heterogeneous Catalysis*; Springer Science & Business Media: 2012.
(2) Fierro, J. L. G. *Metal Oxides: Chemistry and Applications*; CRC Press: 2005.
(3) Hodnett, B. K. *Heterogeneous Catalytic Oxidation: Fundamental and Technological Aspects of the Selective and Total Oxidation of Organic Compounds*; Wiley: 2000.
(4) Doornkamp, C.; Ponec, V. The universal character of the Mars and van Krevelen mechanism. *J. Mol. Catal. A: Chem.* **2000,** *162*, 19-32.
(5) Mars, P.; van Krevelen, D. W. Oxidations carried out by means of vanadium oxide catalysts. *Chem. Eng. Sci.* **1954,** *3*, 41-59.
(6) Vannice, M. A. An analysis of the Mars-van Krevelen rate expression. *Catal. Today* **2007,** *123*, 18-22.
(7) McFarland, E. W.; Metiu, H. Catalysis by doped oxides. *Chem. Rev.* **2013,** *113*, 4391-4427.
(8) Metiu, H.; Chrétien, S.; Hu, Z.; Li, B.; Sun, X. Chemistry of Lewis acid–base pairs on oxide surfaces. *J. Phys. Chem. C* **2012,** *116*, 10439-10450.
(9) Paier, J.; Penschke, C.; Sauer, J. Oxygen defects and surface chemistry of ceria: Quantum chemical studies compared to experiment. *Chem. Rev.* **2013,** *113*, 3949-3985.
(10) Rasmussen, M. D.; Molina, L. M.; Hammer, B. Adsorption, diffusion, and dissociation of molecular oxygen at defected TiO_2(110): A density functional theory study. *J. Chem. Phys.* **2004,** *120*, 988-997.
(11) Ganduglia-Pirovano, M. V.; Sauer, J. Stability of reduced V_2O_5(001) surfaces. *Phys. Rev. B* **2004,** *70*, 1-13.
(12) Ganduglia-Pirovano, M. V.; Hofmann, A.; Sauer, J. Oxygen vacancies in transition metal and rare earth oxides: Current state of understanding and remaining challenges. *Surf. Sci. Rep.* **2007,** *62*, 219-270.
(13) Stiefel, E. I., Molybdenum Compounds. In *Kirk-Othmer Encyclopedia of Chemical Technology*, John Wiley & Sons, Inc.: 2000.

(14) Sebenik, R. F.; Burkin, A. R.; Dorfler, R. R.; Laferty, J. M.; Leichtfried, G.; Meyer-Grünow, H.; Mitchell, P. C. H.; Vukasovich, M. S.; Church, D. A.; Van Riper, G. G., et al., Molybdenum and Molybdenum Compounds. In *Ullmann's Encyclopedia of Industrial Chemistry*, Wiley-VCH Verlag GmbH & Co. KGaA: 2000.
(15) Kresse, G.; Furthmuller, J. Efficient iterative schemes for ab initio total-energy calculations using a plane-wave basis set. *Phys. Rev. B* **1996,** *54*, 11169-11186.
(16) Kresse, G.; Furthmüller, J. Efficiency of ab-initio total energy calculations for metals and semiconductors using a plane-wave basis set. *Comput. Mater. Sci.* **1996,** *6*, 15-50.
(17) Kresse, G.; Hafner, J. Ab initio molecular dynamics for liquid metals. *Phys. Rev. B* **1993,** *47*, 558-561.
(18) Kresse, G.; Hafner, J. Ab initio molecular-dynamics simulation of the liquid-metal–amorphous-semiconductor transition in germanium. *Phys. Rev. B* **1994,** *49*, 14251-14269.
(19) Perdew, J. P.; Burke, K.; Ernzerhof, M. Generalized gradient approximation made simple. *Phys. Rev. Lett.* **1996,** *77*, 3865-3868.
(20) Blöchl, P. E. Projector augmented-wave method. *Phys. Rev. B* **1994,** *50*, 17953-17979.
(21) Grimme, S. Semiempirical GGA-type density functional constructed with a long-range dispersion correction. *J. Comput. Chem.* **2006,** *27*, 1787-1799.
(22) Chrétien, S.; Metiu, H. Electronic structure of partially reduced rutile TiO_2 (110) surface: Where are the unpaired electrons located? *J. Phys. Chem. C* **2011,** *2*, 4696-4705.
(23) Deskins, N. A.; Rousseau, R.; Dupuis, M. Localized electronic states from surface hydroxyls and polarons in TiO_2(110). *J. Phys. Chem. C* **2009,** *113*, 14583-14586.
(24) Di Valentin, C.; Pacchioni, G.; Selloni, A. Electronic structure of defect states in hydroxylated and reduced rutile TiO_2(110) surfaces. *Phys. Rev. Lett.* **2006,** *97*, 166803.
(25) Ganduglia-Pirovano, M. V.; Da Silva, J. L. F.; Sauer, J. Density-functional calculations of the structure of near-surface oxygen vacancies and electron localization on CeO_2(111). *Phys. Rev. Lett.* **2009,** *102*, 1-4.
(26) Li, H. Y.; Wang, H. F.; Gong, X. Q.; Guo, Y. L.; Guo, Y.; Lu, G.; Hu, P. Multiple configurations of the two excess 4f electrons on defective CeO_2 (111): Origin and implications. *Phys. Rev. B* **2009,** *79*, 2-5.
(27) Skorodumova, N. V.; Simak, S. I.; Lundqvist, B. I.; Abrikosov, I. A.; Johansson, B. Quantum origin of the oxygen storage capability of ceria. *Phys. Rev. Lett.* **2002,** *89*, 166601.
(28) Kristoffersen, H. H.; Metiu, H. Reconstruction of low-index α-V_2O_5 surfaces. *J. Phys. Chem. C* **2015,** *119*, 10500-10506.
(29) Sauer, J.; Dobler, J. Structure and reactivity of V_2O_5: Bulk solid, nanosized clusters, species supported on silica and alumina, cluster cations and anions. *Dalton Trans.* **2004**, 3116-3121.
(30) Deskins, N. A.; Rousseau, R.; Dupuis, M. Distribution of Ti^{3+} surface sites in reduced TiO_2. *J. Phys. Chem. C* **2011,** *115*, 7562-7572.